Phase Separation in Monolayers of Pulmonary Surfactant Phospholipids at the Air–Water Interface: Composition and Structure

Bohdana M. Discher,* William R. Schief,# Viola Vogel,# and Stephen B. Hall*§

*Departments of Biochemistry and Molecular Biology, §Physiology and Pharmacology, and §Medicine, Oregon Health Sciences University, Portland, Oregon 97201, and #Department of Bioengineering, University of Washington, Seattle, Washington 98195

ABSTRACT The phase behavior of monolayers containing the complete set of purified phospholipids (PPL) obtained from calf surfactant was investigated as a model for understanding the phase transitions that precede compression of pulmonary surfactant to high surface pressure. During compression, both fluorescence microscopy and Brewster angle microscopy (BAM) distinguished domains that separated from the surrounding film. Quantitative analysis of BAM grayscales indicated optical thicknesses for the PPL domains that were similar to the liquid condensed phase for dipalmitoyl phosphatidylcholine (DPPC), the most abundant component of pulmonary surfactant, and higher and less variable with surface pressure than for the surrounding film. BAM also showed the optical anisotropy that indicates long-range orientational order of tilted lipid chains for the domains, but not for the surrounding film. Fluorescence microscopy shows that addition of DPPC to the PPL increased the area of the domains. At fixed surface pressures from 20–40 mN/m, the total area of each phase grew in proportion with the mol fraction of DPPC. This constant variation allowed analysis of the DPPC mol fraction in each phase, construction of a simple phase diagram, and calculation of the molecular area for each phase. Our results indicate that the phase surrounding the domains is more expanded and compressible, and contains reduced amounts of DPPC in addition to the other phospholipids. The domains contain a mol fraction for DPPC of at least 96%.

INTRODUCTION

The structure of the interfacial film of pulmonary surfactant is a critical determinant of its physiological function. Pulmonary surfactant is the mix of lipids and proteins that coats the alveolar air spaces. It adsorbs to the surface of the thin liquid layer that lines the alveoli, and the resulting film lowers interfacial tension and stabilizes small alveoli. During the expiratory phase of the respiratory cycle, the decreasing alveolar surface area compresses the film, and measurements in the lung indicate that its surface pressure achieves high values approaching 70 mN/m (Schürch, 1982). Lung surfactant's physiological function then depends on the formation of a film that remains stable at such high pressures without collapse from the interface. Most investigators have attributed this stability to the presence of a highly ordered liquid-condensed (LC) phase (Keough, 1992). The most prevalent component of surfactant, dipalmitoyl phosphatidylcholine (DPPC), occurs as the LC phase in single-component monolayers at physiologic temperatures and can achieve the pressures measured in the lung. This constituent, however, represents only a third of surfactant (Kahn et al., 1995), and both the structure and the composition of the functional film in situ remain uncertain.

We have undertaken studies of the phase behavior of surfactant monolayers at pressures below the equilibrium spreading pressures of approximately 45 mN/m. Phase behavior under these conditions provides important information for understanding the development of the structure and composition of the functional film at higher pressures. Our studies emphasize the full complexity of the surfactant mixture both to complement results with the simple model systems used by others (e.g., Nag and Keough, 1993; Lipp et al., 1996) and because the diverse set of components may be functionally important. We previously used microscopic methods to show phase separation in monolayers of extracted calf surfactant (calf lung surfactant extract, CLSE) (Discher et al., 1996). Both fluorescence microscopy and Brewster angle microscopy (BAM) demonstrated a coexistence of condensed and expanded phases over a wide range of surface pressure. Several characteristics of the condensed phase suggested that it is enriched in DPPC. Nag and coworkers have recently reported similar phase separation in films of extracted porcine surfactant (Nag et al., 1998).

The studies reported here extend our prior investigations to analyze in more detail the composition and structure of the two phases identified previously. In the current experiments, we have worked with a simplified system containing the complete set of purified phospholipids (PPL) obtained from calf surfactant without the proteins or cholesterol. PPL contains 33 mol% DPPC (Kahn et al., 1995), and the isotherm and phase behavior of PPL are in many respects similar to CLSE (Discher et al., 1999). To address the composition of the domains, we have now used fluorescence microscopy to monitor the area of each phase in response to DPPC added to the PPL. A simple but exact mathematical analysis determines the content of an added constituent in each coexisting phase if the changes in area are proportional to the amount added. In these studies, the linear relationships between the area of each phase and the added DPPC provides their content of DPPC at different

Received for publication 16 March 1999 and in final form 30 June 1999.

Address reprint requests to Stephen B. Hall, Mail Code NRC-3, Oregon Health Sciences University, Portland, OR 97201-3098. Tel.: 503-494-6667; Fax: 503-494-6670; E-mail: sbh@ohsu.edu.

0006-3495/99/10/2051/11 $2.00

surface pressures. BAM provides additional structural information. Quantitative analysis of BAM grayscales for expanded and condensed phases allows comparison of the optical thickness in monolayers containing pure DPPC, PPL, and two mixtures of PPL with added DPPC. In addition, we compare long-range orientational order of tilted lipid chains in the condensed phase between pure DPPC and PPL domains. Our results provide a self-consistent picture indicating that compressed monolayers of the surfactant phospholipids contain condensed domains highly enriched in DPPC.

MATERIALS AND METHODS

Materials

Phosphatidylglycerol (PG) derived from egg yolk lecithin and DPPC (>99% pure) were obtained from Sigma Chemical Company (St. Louis, MO) and used without further characterization or purification. The following compounds (>99% pure) were purchased from Avanti Polar Lipids (Alabaster, AL): rhodamine-dipalmitoyl phosphatidylethanolamine (Rh-DPPE) labeled at the head group (*N*-(Lissamine rhodamine B sulfonyl)-1,2-dihexadecanoyl-*sn*-glycero-3-phosphoethanolamine); 1-palmitoyl-2-myristoyl-*sn*-glycero-3-phosphocholine (PMPC); 1-palmitoyl-2-oleoyl-*sn*-glycero-3-phosphocholine (POPC); 1-palmitoyl-2-palmitoleoyl-*sn*-3-phosphocholine (PPoPC).

The PPL were separated from CLSE provided by Dr. Edmund Egan of ONY, Inc. (Amherst, NY). CLSE is obtained by lavaging freshly excised calf lungs, removing cells from the lavage fluid by low-speed centrifugation, pelleting the large surfactant aggregates from the cell-free lavage at $12{,}500 \times g$ for thirty min, and extracting the resuspended pellet (Notter et al., 1983). Column chromatography then separates the CLSE into distinct peaks for the surfactant proteins, phospholipids, and cholesterol (Takahashi and Fujiwara, 1986). Pooling the appropriate fractions provides the PPL without proteins or cholesterol (Hall et al., 1994). The original published protocol used a column that incompletely separated the proteins from the phospholipids and required two passes through the column to obtain PPL. Substitution of a longer column accomplishes the complete separation during a single elution. PPL obtained with this procedure contains 33 mol% DPPC, 15% PPoPC, 11% POPC, 10% PMPC, and 9% anionic phospholipids consisting of a complex mixture of phosphatidylinositols and phosphatidylglycerols (Kahn et al., 1995). Additional constituents include minor PCs and PEs, each representing less than 3% of the mixture.

Mixtures of PPL with DPPC were prepared to vary the content of DPPC while maintaining the other constituents in native ratios relative to each other. These mixtures contained the following amounts of DPPC, expressed as total mol% DPPC (and added mol%, given in parentheses): 33% (0%); 40% (10%); 50% (25%); 60% (40%); 70% (55%); 80% (70%); 90% (85%); 100% (100%).

A synthetic replica of native PPL containing the major constituents was also prepared as a control using commercially available phospholipids. This mixture contained 11 mol% PG, 19% PPoPC, 14% POPC, 13% PMPC, and 42% DPPC to preserve the native ratios of these components with each other. A second synthetic mixture contained the same components in the same ratios except that DPPC was omitted. PG converted from egg lecithin provided a readily available source of anionic phospholipids with pairs of mixed acyl groups to substitute for the anionic compounds in pulmonary surfactant.

The subphase for all experiments contained 10 mM HEPES pH 7.0, 150 mM NaCl, 1.5 mM $CaCl_2$ (HSC). Water for these studies was first distilled and then purified by using systems obtained from Millipore (Bedford, MA) or Barnstead (Dubuque, IA). All glassware was acid-cleaned. All solvents were at least reagent-grade and contained no surface active stabilizing agents.

Methods

Biochemical assays

Phospholipid concentrations were determined by measuring the phosphate content (Ames, 1966) of measured aliquots.

Fluorescence microscopy

This method detects contrast between regions of the film that differ in their solubility of a phospholipid probe labeled with a fluorescent chromophore (Lösche et al., 1983; Peters and Beck, 1983; McConnell et al., 1984). The large rhodamine group on the Rh-DPPE probe used for these studies lowers its solubility in condensed phases. Images were obtained through a Nikon epifluorescence microscope focused on the surface of a Langmuir trough. The microscope uses infinity optics and a 100× super-long working distance objective assembled on a custom-built stand. The Langmuir trough confines films within a constant-perimeter vertical Teflon ribbon (Labcon, Darlington, UK) that linearly varies the confined area by reconfiguration of the ribbon (Tabak and Notter, 1977). The maximum area is 532 cm^2, and the subphase volume is approximately one liter. A computer controls movement of the barrier and processes measurements of the surface pressure and surface area by means of the graphical interface program LabView (National Instruments, Austin, TX). Phospholipid solutions in chloroform contained 0.1 mol% Rh-DPPE unless specified otherwise. Solutions were spread in volumes of approximately 80 μL to an initial molecular area of 120 $Å^2$/molecule. After 10 min to allow for evaporation of the solvent, films were compressed at 3 $Å^2$/molecule/min. The temperature of the subphase for these experiments was maintained at 20°C by water pumped through the base of the trough.

Images were obtained by a Hamamatsu C2400 SIT camera, and then either recorded by VCR for later analysis or captured directly to computer (Macintosh IIci, Apple, Cupertino, CA) by means of frame grabber (LG-3, Scion Corp., Frederick, MD). A C-shaped Teflon mask placed directly in the subphase minimized movement of the monolayer (Meller, 1988; Grainger et al., 1989). Images recorded inside and outside the mask ensured that it created no artifacts. Images were captured and analyzed using the program Image, developed at the National Institutes of Health and available from the public domain on the internet at http://rsb.info.gov/nih-image. The fraction of interfacial area occupied by the nonfluorescent domains was calculated by counting pixels with grayscale below assigned threshold values. At least three images were analyzed from different parts of the film in each of four experiments to obtain each fractional area.

Analysis of response to compositional variation

To investigate the extent to which the nonfluorescent domains contain DPPC, we measured changes in the area of each coexisting phase in response to added DPPC. Analysis of these results required an expression relating the area of each phase to the amount of a single compound added to the mixture. If the total number of molecules in the film is n, and the number for the condensed and expanded phases are n_c and n_e, respectively, then

$$n = n_c + n_e.$$

Our complex mixtures contain numerous constituents, each of which can partition differently between the two phases. At any given surface pressure, the mol fraction X^i of the constituent i in the complete film can be expressed in terms of its mol fractions for the two phases, X^i_c and X^i_e, by

$$n \cdot X^i = n_n \cdot X^i_c + n_e \cdot X^i_e.$$

These relationships lead directly to the lever rule,

$$\frac{n_c}{n_e} = \frac{(X^i - X^i_e)}{(X^i_c - X^i)},$$

and also provide a relationship between composition and the fraction f of all molecules in each phase,

$$f_c \equiv \frac{n_c}{n} = \frac{(X^i - X^i_e)}{(X^i_c - X^i_e)}, \qquad f_e \equiv \frac{n_e}{n} = \frac{(X^i_c - X^i)}{(X^i_c - X^i_e)}.$$

In terms of our experimental measurements, the total area of the condensed phase is given by

$$\phi_c \cdot \tilde{A} = f_c \cdot \tilde{A}_c,$$

where ϕ_c is the fraction of the interface occupied by the condensed phase, $\tilde{A}$ is the molecular area of the entire film, and $\tilde{A}_c$ is the average molecular area within the condensed phase (Knobler, 1990). Substitution for f_c and f_e then yields

$$\phi_c \cdot \tilde{A} = \tilde{A}_c \cdot \frac{(X^i - X^i_e)}{(X^i_c - X^i_e)} \tag{1}$$

for the condensed phase and

$$\phi_e \cdot \tilde{A} = (1 - \phi_c) \cdot \tilde{A} = \tilde{A}_e \cdot \frac{(X^i_c - X^i)}{(X^i_c - X^i_e)} \tag{2}$$

for the expanded phase. These expressions relate the areas of each phase to the compositions for any particular constituent.

When phase areas vary linearly with X^i at a fixed surface pressure, this relationship provides a simple approach for calculating the compositions of each phase. According to Eq. 1, plots of $\phi_c \cdot \tilde{A}$ versus X^i will have a slope of $\tilde{A}_c/(X^i_c - X^i_e)$ and an ordinate intercept of $-\tilde{A} \cdot X^i_e/(X^i_c - X^i_e)$. The ratio of $-$intercept/slope provides X^i_e. From Eq. 2, the comparable ratio for plots of $\phi_e \cdot \tilde{A}$ yields X^i_c. This method then determines the content of component i in each phase (X^i_c, X^i_e) at a given surface pressure.

Brewster angle microscopy

BAM examined films containing no added fluorescent probes. BAM derives contrast within a film from differences in reflectivity to p-polarized light incident at Brewster's angle for the clean air–water interface (Hénon and Meunier, 1991; Hönig and Möbius, 1991). The previously described home-built instrument used in these studies (Frey et al., 1996) was mounted on an x–y translation stage (Newport Corp., Irvine, CA) and used to image the surface of the same Langmuir trough used for the fluorescence measurements. The air–monolayer–water interface was illuminated at $\theta \approx 53.1°$ by a laser beam polarized (Glan–Thompson) in the plane of incidence (p-polarized), and a lens system focused an image onto a charge coupled device camera. An analyzer (Glan–Thompson polarizer on the output arm) of variable orientation was present for all measurements. In experiments to detect anisotropy in the reflected images, the analyzer was rotated to specific angles in opposite directions from p-polarization. Images from the camera were captured directly by computer.

Grayscale values are linearly proportional to the reflectance of interfacial structures to p-polarized light, and were reproducible between experiments to within ± 5 units out of 256. Each reported value of grayscale represents the mean of a Gaussian fit to a grayscale histogram taken within either condensed or expanded phases in one image. Grayscale values were measured with the analyzer set to p-polarization. Data shown here are representative of at least three experiments. Since the laser intensity is stable to within $\pm 2\%$, and we maintained fixed camera gain and offset for all experiments, quantitative measurements of grayscale proved to be reproducible if the reflected beam was maintained on the optical axis of the microscope. Deviations from this central alignment cause an inhomogeneous image illumination. Water was added by pipette to counter the effect of evaporation. This proved sufficient to maintain the surface height to within approximately ± 20 μm. The grayscale of the plain air–buffer interface, which corresponds to zero reflectivity, was 18 arbitrary units.

Statistics

Data are stated as mean $\pm$ S.D. unless stated otherwise. The standard error of the slope and intercept for linear fits of the area of each phase to the mol fraction of DPPC (see Fig. 5) were calculated using the program Igor Pro (WaveMetrics, Lake Oswego, OR). Assuming that the covariance between the slope m and the intercept b is zero, then the standard error σ_r for the ratio $r = b/m$ is given by

$$\sigma_r = r \cdot \left[\left(\frac{\sigma_b}{b} \right)^2 + \left(\frac{\sigma_m}{m} \right)^2 \right]^{1/2}.$$

where σ_b^2 and σ_m^2 are the variances for the intercept and slope, respectively (Bevington and Robinson, 1992) .

RESULTS

Compression of monolayers containing the surfactant phospholipids induced the separation of two phases. Both fluorescence microscopy and BAM distinguished domains that become visible in films of PPL at approximately 6 mN/m and grew as surface pressure increased. The domains were dark by fluorescence microscopy, demonstrating exclusion of the fluorescent probe from these areas (Fig. 1). In BAM, domains appeared bright, indicating greater optical thickness than the surrounding film (Fig. 2). We have shown previously that the initial convoluted shape of the PPL domains represented nonequilibrium forms (Discher et al., 1999). After equilibration for several hours, the domains converted to more circular shapes. The total nonfluorescent area decreased 5% during relaxation of the domains over a period of 6 h.

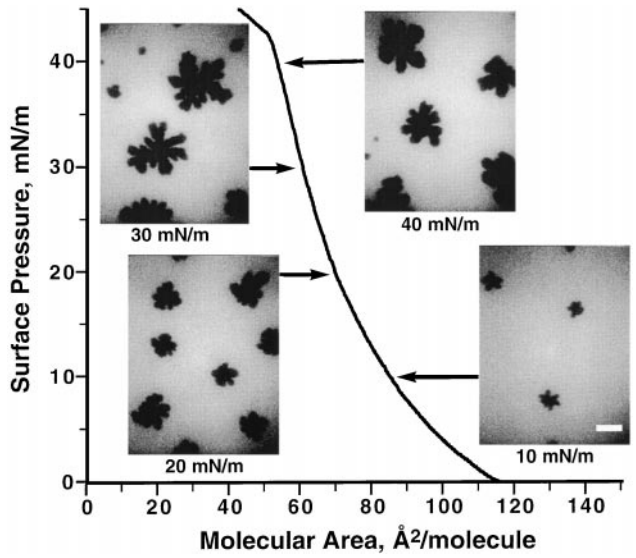

FIGURE 1 Surface pressure–area isotherm with epifluorescence images for PPL from calf surfactant. Chloroform solutions of PPL containing 0.1% Rh-DPPE were spread to an initial molecular area of 150 Å^2/molecule on a subphase of HSC at 20°C. The isotherm was recorded during continuous compression at 3 Å^2/molecule/min. Fluorescence images were recorded in separate experiments from static films after compression at the same rate to the designated pressure. Images are representative of greater than 50 experiments. Scale bar represents 50 μm.

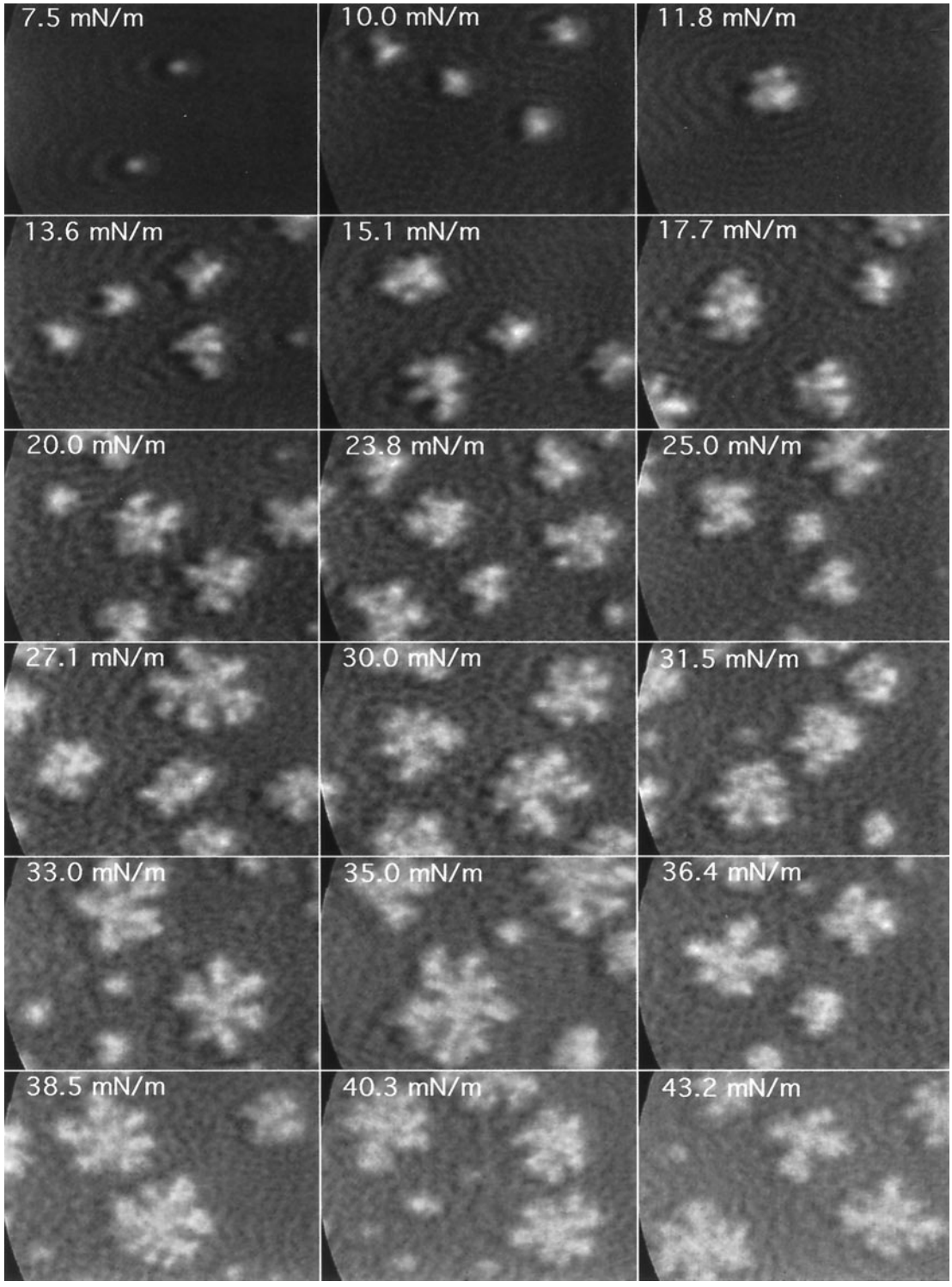

FIGURE 2 Brewster angle micrographs of PPL monolayers. Analyzer in the reflected beam is set to p-polarization for all images. Contrast in all images has been enhanced identically to preserve the relative grayscale. Solutions of PPL in chloroform were spread on a subphase of HSC at room temperature and compressed at 1.4 $Å^2$/molecule/min. Images were obtained during continuous compression at the surface pressures indicated, and are 200 $\times$ 150 μm in size.

Our prior results with CLSE (Discher et al., 1996) and with PPL (Discher et al., 1999) suggested that the domains are enriched in DPPC relative to the surrounding film. In that case, altering the amount of DPPC in the film should change the total area of the domains. To test this hypothesis, we mixed PPL with different amounts of DPPC. The nonfluorescent fraction of the interface increased with added DPPC (Fig. 3). Domains emerged between 4 and 6 mN/m in

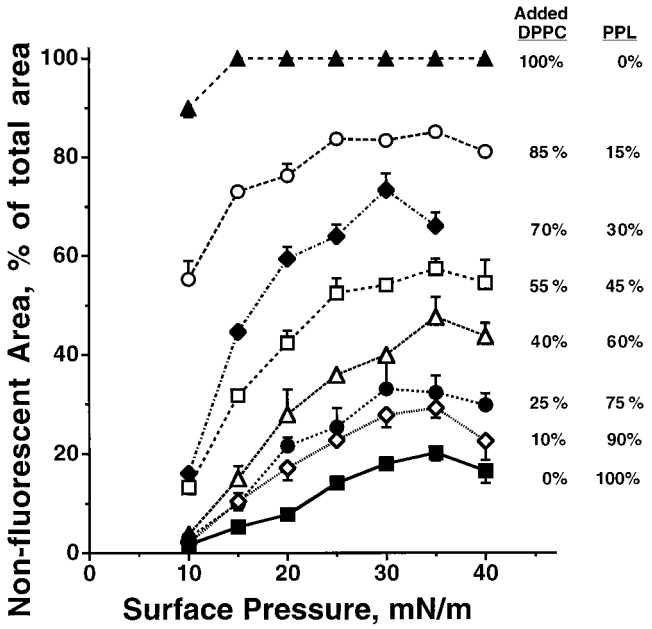

FIGURE 3 Variation of nonfluorescent area with surface pressure for different mixtures of PPL with added DPPC. Images obtained on static films were analyzed to determine the percentage of the interface occupied by the nonfluorescent domains. DPPC-PPL mixtures are described in terms of the amount of added DPPC expressed as the mol fraction of total phospholipid. At least three images were analyzed from different parts of the film in each of four experiments to obtain each data point. Error bars indicate S.D.

all PPL-DPPC mixtures and then grew to a maximum area at 30–35 mN/m before declining at 40 mN/m (Fig. 3). At each surface pressure for which fluorescence micrographs were obtained, more DPPC produced a larger nonfluorescent area (Fig. 3). We also tested synthetic replicas of PPL, with and without DPPC, prepared from commercially available individual phospholipids to determine if domains would appear in the absence of DPPC. PPL contains four major phosphatidylcholines that constitute approximately 70% of the mixture (Kahn et al., 1995). Films containing these components in the appropriate ratios with PG produced nonfluorescent domains. When DPPC was omitted from these mixtures, microscopy detected no separation of phases. Neither the requirement of the nonfluorescent phase for DPPC nor its growth in response to added DPPC prove that the domains contain only DPPC. Domains composed strictly of other constituents might still incorporate DPPC when more of that compound is added to the film. Domains that vanish in the absence of DPPC might still contain other compounds such as PMPC or DPPG if the nonfluorescent phase requires a minimum content of disaturated compounds in general rather than specifically DPPC. The absence of the domains, however, in films containing no DPPC and their enlargement in response to added DPPC both fit with the hypothesis that the nonfluorescent phase is enriched in that compound.

The micrographic images allowed quantitation of the total area occupied by each phase. The fraction of the interface, ϕ_c and ϕ_e, occupied by the condensed and expanded phases, obtained from the fluorescence micrographs (Fig. 3), multiplied by the average molecular area $\tilde{A}$ for the entire film, obtained from the compression isotherms (Fig. 4), gave the area of each phase. The fluorescence images were recorded at specific surface pressures, and the total areas at these fixed pressures were plotted as a function of the DPPC mol fraction (Fig. 5). The relationships between the phase areas and DPPC mol fraction of the monolayer changed with pressure. At 10 and 15 mN/m, the plots were nonlinear; the area of each phase initially changed little in response to added DPPC, but then increased steeply. At higher pressures, both the fluorescent and the nonfluorescent areas varied linearly with the content of DPPC (Fig. 5).

This linear response at pressures above 15 mN/m allowed direct calculation of the DPPC composition for the two phases. At a fixed surface pressure, the variation of the total area for one phase in response to a constituent added to the film depends on the mol fraction of that constituent in each phase and in the film, and on the molecular area of that phase. If the variation is linear, however, the ratio of −intercept/slope gives the mol fraction of the added constituent in the other phase (see Methods). Values of X_c^{DPPC} and X_e^{DPPC}, the mol fractions for DPPC in each phase, were then calculated from the linear plots of phase area versus X^{DPPC}, the mol fraction in the entire film, at each surface pressure above 15 mN/m. These values allowed construction of a simple phase diagram (Fig. 6). The surface pressures at which the domains first appeared for the different mixtures

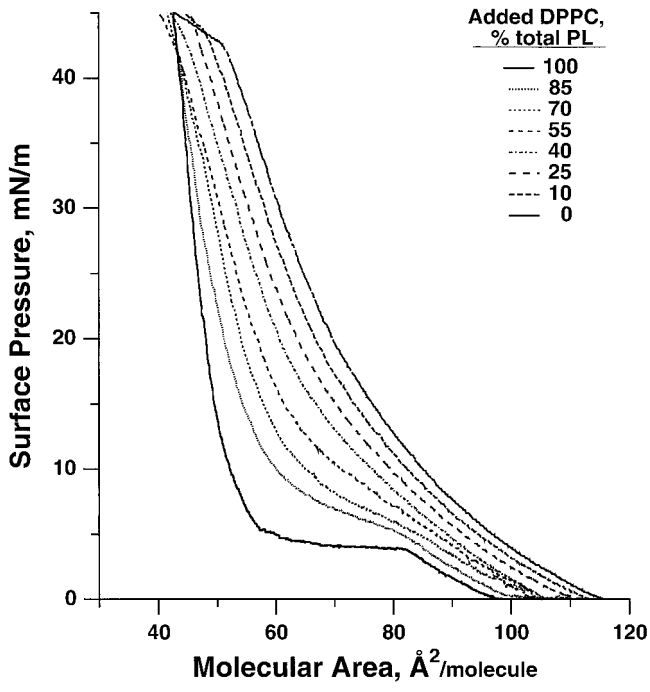

FIGURE 4 Compression isotherms for mixtures of PPL and DPPC. Mixtures containing 0.1% Rh-DPPE were spread in chloroform to 120 Å^2/molecule on a subphase of HSC and compressed continuously at 3 Å^2/molecule/min.

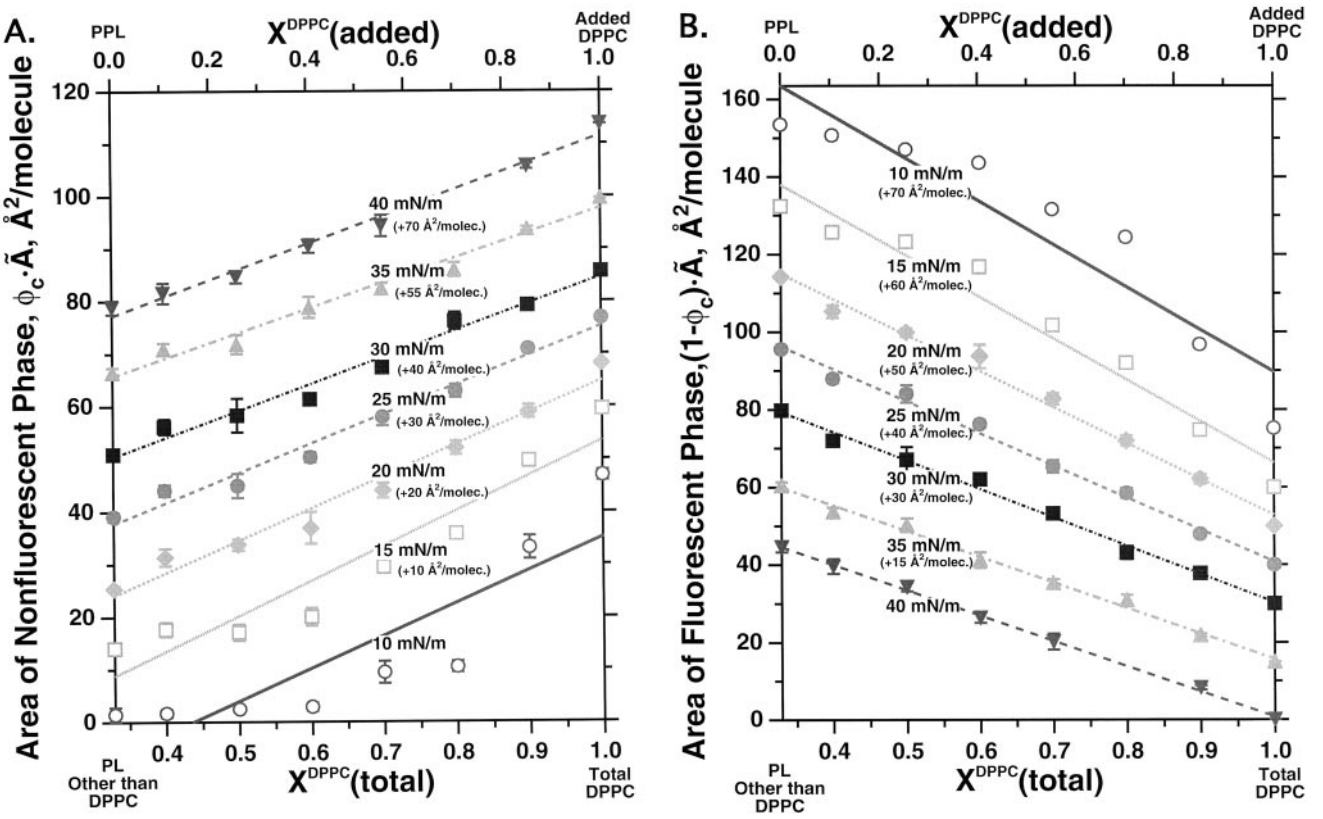

FIGURE 5 Variation of the total area of each phase with the content of DPPC at incremental surface pressures. (*A*) Area of the nonfluorescent domains. (*B*) Area of the surrounding fluorescent film. Areas were calculated as the product of the fraction of the interface occupied by each phase, ϕ_c or $(1 - \phi_c)$, times $\tilde{A}$, the average molecular area of the film. X^{DPPC}(added) on the top axis is the mol fraction of the DPPC added to the DPPC-PPL mixtures. X^{DPPC}(total) is the mol fraction of total DPPC, including DPPC endogenous to PPL using the previously determined content of 33% DPPC in PPL (Kahn et al., 1995). The line in each case represents the linear least squares fit to the data. For clarity of presentation, areas are offset by the increment in Å^2/molecule indicated for each set of data. Error bars indicate ±S.D.

defined the lower boundary of the coexistence region. The compositions obtained at specific surface pressures from the plots of $\phi \cdot \tilde{A}$ versus X^{DPPC} for each phase defined the lateral boundaries. The values from this analysis indicated that the coexisting fluorescent phase contained mostly phospholipids other than DPPC. The limited content of DPPC in this phase fell from 26 ± 5% at 20 mN/m to a minimum of 11 ± 4% at 35 mN/m before increasing to 19 ± 4% at 40 mN/m. The nonfluorescent phase contained 103 ± 5% DPPC at 20 mN/m, 100 ± 4% at 30 mN/m, and 100 ± 2% at 40 mN/m. Within the error of the analysis, the domains at all pressures above 15 mN/m contained no less than 96% DPPC.

This analysis also provided values for the molecular areas, $\tilde{A}_c$ and $\tilde{A}_e$, for each phase (Fig. 7). Above 15 mN/m, the constant variation of the area for a phase in response to a constituent added to the film required not only a constant content of that constituent in each phase, but also that the molecular area of that phase must be fixed (see Methods). The values of $\tilde{A}_c$ and $\tilde{A}_e$, obtained from Eqs. 1 and 2 using the calculated mol fractions of DPPC in each phase, were therefore averaged at each surface pressure for the different mixtures. These average values of $\tilde{A}_c$ and $\tilde{A}_e$ at different surface pressures allowed construction of compression isotherms for each phase (Fig. 7). The molecular areas of the domains calculated by this procedure fit well with measured isotherms for pure DPPC (Fig. 7). The surrounding film, containing the same phospholipids as PPL except for a reduced content of DPPC, had areas shifted to values slightly larger than for PPL (Fig. 7). These data agreed with the phase diagram to present a self-consistent view of the phase behavior for the surfactant phospholipids, and fit with the finding that the domains contained mostly DPPC.

BAM provides an additional test of the extent to which the PPL domains contained mostly DPPC by measuring grayscale values in a reproducible manner. The grayscale values and their variation with surface pressure are then compared for each phase between different monolayers. Quantitative grayscales were extracted from images for PPL, DPPC, and for two mixtures of PPL-DPPC containing 50 and 70% added DPPC. These measurements required care to achieve the same interfacial level for different experiments and to maintain that level during the course of an experiment. Grayscale values then proved reproducible between experiments to within ±5 units on a scale of 256 (Fig. 8 *A*). These results established that BAM could produce

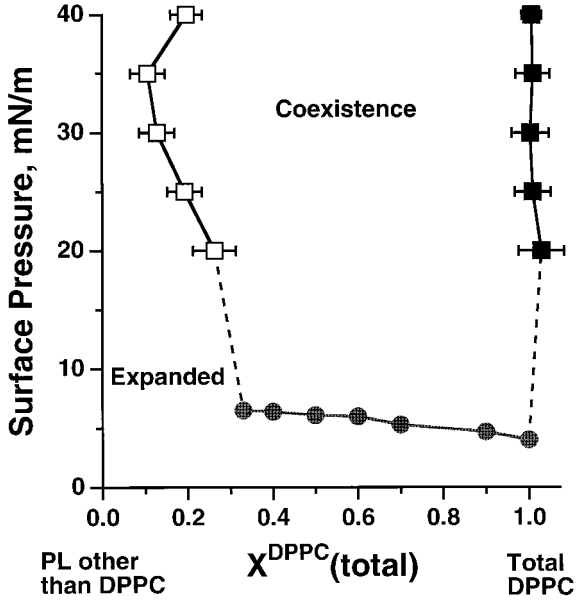

FIGURE 6 Phase diagram for PPL with respect to content of DPPC. X^{DPPC}(total) is the mol fraction of total DPPC, including material both added and endogenous to PPL. Gray circles are points determined directly from the surface pressures at which domains first emerged for the different mixtures. Squares indicate the compositions calculated for the fluorescent (*empty squares*) and nonfluorescent (*filled squares*) phases from the variation in areas with composition at specific surface pressures (Fig. 7). Error bars indicate ±S.D. calculated according to standard rules for propagation of errors (Bevington and Robinson, 1992). Data at 10 and 15 mN/m, where the relationships between phase area and content of DPPC were nonlinear, are omitted from this diagram. Dotted lines instead connect the two sets of established points. "Expanded" indicates the region of the homogeneously fluorescent monolayer. "Coexistence" indicates the conditions under which nonfluorescent domains are present together with the surrounding fluorescent monolayer.

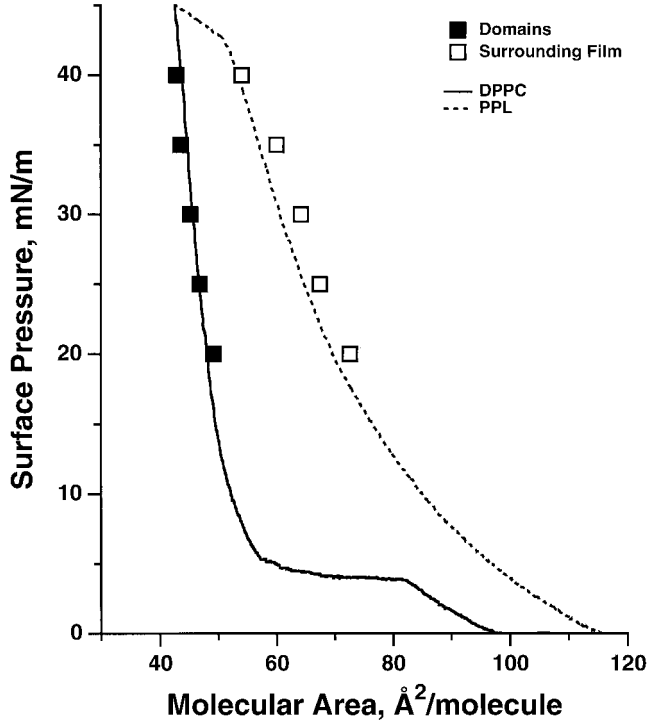

FIGURE 7 Surface pressure–area isotherm for each phase in mixed monolayers of DPPC-PPL. Values of the molecular area for each phase were calculated from the phase diagram and microscopic measurements and averaged over the series of DPPC-PPL mixtures at each surface pressure. Filled symbols give values for the domains, and empty symbols for the surrounding film. Continuous isotherms measured for pure DPPC and for PPL are shown for comparison.

grayscale values that could serve as a quantitative characteristic for comparison between different monolayers.

Grayscale measurements demonstrated several similarities between the phases in monolayers of DPPC and in films containing PPL (Fig. 8 *B*). First, the domains in PPL and in the two PPL-DPPC mixtures were more reflective than the surrounding phase, just as the LC regions of DPPC monolayers were more reflective than the liquid-expanded (LE) phase. For surface pressures between 0 and 40 mN/m, the grayscale of the condensed phase in all four systems ranged from 120 to 141, whereas the expanded phase produced lower values between 33 and 79. The grayscale for LE DPPC itself was 36 ± 2. Second, the domains in films containing PPL had grayscale values similar in magnitude to the LC phase of DPPC. Grayscale values of the domains in the two PPL-DPPC mixtures (130 ± 5 for PPL:DPPC 30:70, and 132 ± 5 for PPL:DPPC 50:50 at 20 mN/m) were identical to values for LC DPPC (130 ± 5) within experimental error, whereas the values for PPL (121 ± 5) were slightly lower. Third, LC DPPC and the domains in films containing PPL showed similarly limited variation in grayscale during compression, which was significantly less than for the surrounding film (Fig. 8 *B*). Among the four systems, the average slope of the linear fits of grayscale versus surface pressure for the condensed phase was 0.36 ± 0.15, but greater by threefold (1.00 ± 0.09) for the expanded phase (Fig. 8 *B*). For the LE phase of DPPC, the termination of the coexistence plateau limited measurements to surface pressures below 6 mN/m. The grayscale for LE DPPC remained constant across the plateau, consistent with a first-order phase transition in a single component system.

BAM also allows detection of long-range tilt orientational order within the film (Hönig et al., 1992; Weidemann and Vollhardt, 1995). The hydrocarbon chains within condensed phases of surface films are often tilted from the interfacial normal. The in-plane orientation of the tilted chains differs for different regions of the condensed phase. BAM can resolve this orientational order because of the different reflectivities of regions with different orientations (Maruyama et al., 1996). Use of an analyzing polarizer in the reflected beam enhances detection of the optical anisotropy. When imaging an isotropic phase, rotation of the analyzer in opposite directions from *p*-polarization produces a symmetric reduction of the image grayscale according to $\cos^2\alpha$, where α is the angle between the analyzer and the incident plane. When imaging a tilted phase, however, an analyzer scan will produce a grayscale variation proportional to $\cos^2(\alpha - \alpha_0)$, where the shift α_0 depends on the

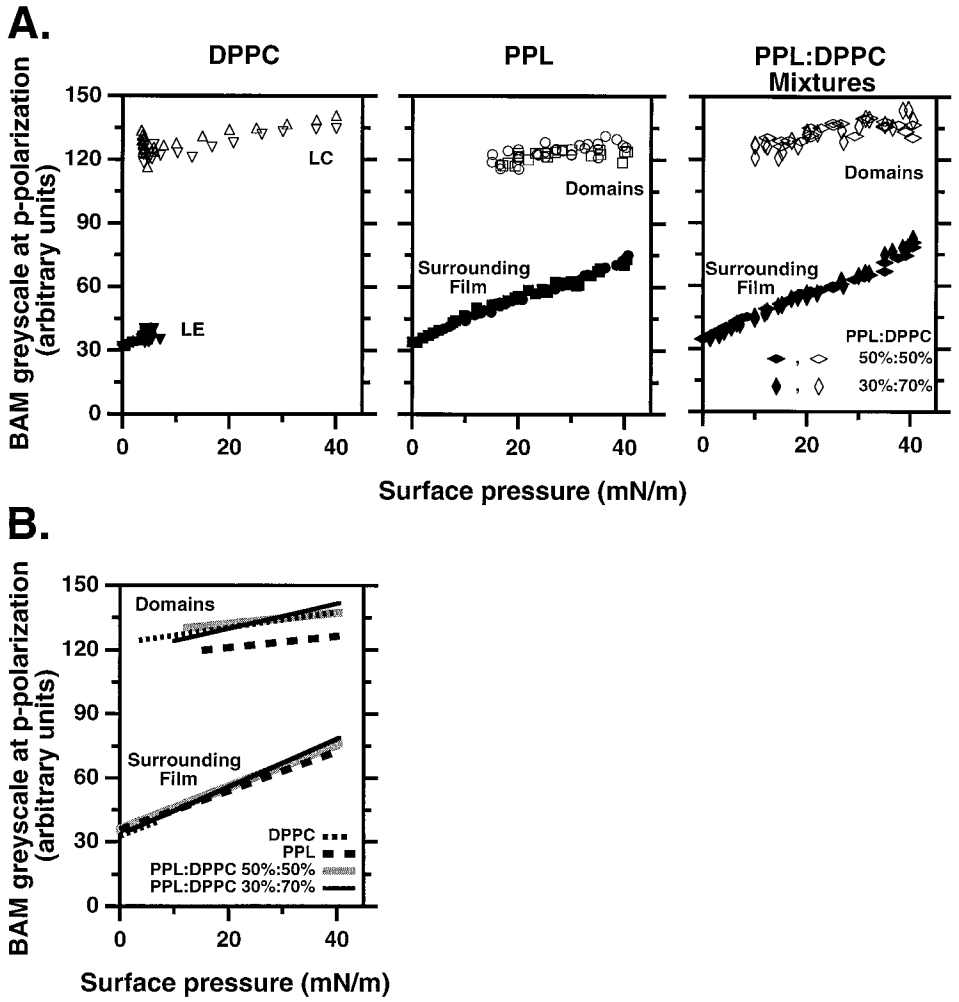

FIGURE 8 Variation of grayscale in Brewster angle micrographs. Chloroform solutions of phospholipids were spread on HSC subphase to an initial molecular area of at least 120 Å^2/molecule. Films were compressed at 1.4 Å^2/molecule/minute. (*A*) Grayscale values plotted versus surface pressure for different monolayer phases in the four systems: DPPC, PPL, PPL:DPPC 50%:50% (mol:mol), and PPL:DPPC 30%:70%. Open and filled symbols represent the condensed and expanded phases, respectively. Different symbols indicate results from two experiments for DPPC and PPL, and for the two compositions for the DPPC-PPL mixtures. The grayscale of the plain air–buffer interface, which corresponds to zero reflectivity, was 17.5. (*B*) Linear least squares fits to the four sets of grayscale values in Fig. 8 *A*.

molecular orientation. Therefore, with the exception of regions oriented within the plane of incidence, a tilted region viewed with opposite orientations of the analyzer about *p*-polarization will show different reflectivities.

Our experiments detected anisotropy for the domains in both DPPC and PPL (Fig. 9). Opposite rotations of the analyzer produced different effects on grayscale within distinct regions of the domains. For the domains in DPPC, the contrast varied continuously along the triskelion arms. The progressive variation was not evident in the irregularly shaped domains in PPL, but opposite analyzer rotations again showed regions with different effects on reflected intensity, indicating long-range tilt orientational order. In contrast, the film surrounding the domains showed no anisotropy. Rotation of the analyzer through an angle $\pm\alpha$ away from *p*-polarization reduced the grayscale for these regions by $\cos^2\alpha$, as expected for an isotropic phase.

DISCUSSION

Understanding the phase behavior of pulmonary surfactant in the range of low surface pressure is a prerequisite to establish the molecular mechanisms by which surfactant films stabilize alveoli at high surface pressures. These studies show that compression of monolayers containing the complete set of PPL obtained from calf surfactant induces the separation of microscopic domains from the surrounding film. Several characteristics suggest that the domains contain mostly DPPC. They have the appearance of a condensed phase, excluding fluorescent probe in fluorescence micrographs (Fig. 1) and showing increased reflectivity by BAM (Fig. 2). DPPC is the only major constituent of calf surfactant that, by itself, can form a condensed film under the conditions used in our experiments (Kahn et al., 1995). In mixtures of synthetic compounds prepared to replicate the composition of PPL, domains are absent if DPPC is omitted. Titration experiments show that addition of DPPC to PPL monolayers increases the total area of the domains (Fig. 5). Above 15 mN/m, the increase in area is proportional to the amount of added DPPC. Quantitative analysis of this linear increase indicates that the mol fraction of DPPC within the domains is 1.00 $\pm$ 0.04. The other phospholipids are sequestered into the surrounding film. Some DPPC remains outside the domains, and its solubility in the surrounding film varies with surface pressure (Fig. 6). In

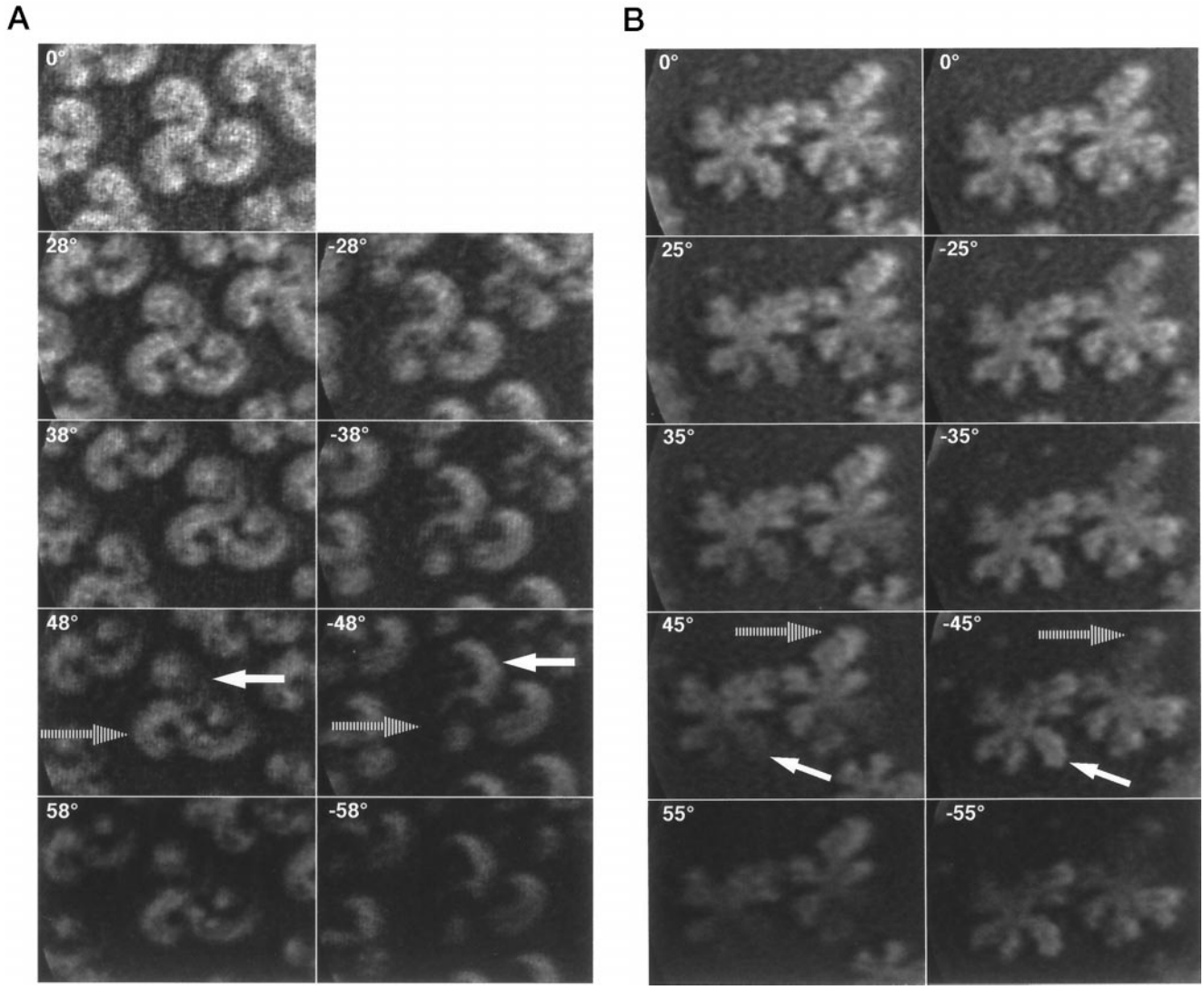

FIGURE 9 Anisotropy in Brewster angle micrographs. An analyzer in the reflected beam was rotated through the angle from p polarization indicated for each micrograph. (*A*) DPPC at 5 mN/m. (*B*) PPL at 30 mN/m. Solid and broken arrows identify examples of regions that show different changes in grayscale with opposite rotations of the analyzer. Images have been contrast enhanced in an identical manner so the relative grayscale is preserved, and are 200 × 150 μm in size.

contrast, the mol fraction of DPPC in the domains is constant (Fig. 6).

Both microscopic methods provide quantitative information that fits the behavior predicted from the compositional analysis. Grayscale measurements for the domains in BAM images of monolayers containing PPL or DPPC-PPL mixtures agree well with values for LC DPPC (Fig. 8). The surrounding film has values that are significantly smaller. The variation of grayscale with surface pressure for the domains in films containing PPL is comparable to that of LC DPPC, and significantly less than for the film surrounding the domains (Fig. 8). Analysis of the variation of nonfluorescent area in response to added DPPC allowed calculation of the molecular area both within the domains and in the surrounding film. For any surface pressure, the PPL domains have the same area/molecule as pure DPPC (Fig. 7). Molecular areas for the surrounding film are considerably larger. This difference in molecular areas provides definitive evidence that the phase transition is first order despite the broad range of surface pressures over which it occurs. The multiple components of the mixture release the constraint of the Gibbs phase rule that such a transition for a single component film must occur at a fixed pressure.

Despite these similarities between the domains in PPL and pure DPPC, there are subtle differences. First, the optical anisotropy appears to be different. Although BAM shows that the PPL domains display anisotropy that indicates the long-range order of tilted acyl chains expected of a LC phase, the pattern of anisotropy appears to be different than for DPPC. Our measurements for DPPC show the gradual shift in anisotropy along the triskelion arms (Fig. 9 *A*) that has been observed previously using polarized fluorescence (Moy et al., 1986, 1988) and BAM (Weidemann and Vollhardt, 1995, 1996). This pattern indicates a

gradual variation of the in-plane molecular orientation and is distinct from the behavior of compounds such as dimyristoyl phosphatidylethanolamine (DMPE), for which the in-plane projection appears to change in discrete jumps (Weidemann and Vollhardt, 1995). The domains in PPL appear to have a homogeneous brightness within individual branches (Fig. 9 *B*), suggesting a common orientation within each branch, behavior more similar to that of DMPE than of DPPC. A difference in the pattern of collective chain tilt would be consistent with a different composition. The second difference between the domains for PPL and DPPC is their shape. The domains for PPL at equilibrium are circular (Discher et al., 1999) and lack the triskelion or kidney-bean features that originate from the chiral nature of DPPC (McConlogue and Vanderlick, 1997). The subtle differences in both the pattern of anisotropy and the shape of the domains may reflect the presence of small amounts of constituents other than DPPC within the PPL domains. Our quantitative analysis by fluorescence microscopy indicates that this other material should have a mol fraction <0.04.

Our results provide more specific information concerning the nature of the domains in surfactant films than was available previously. Prior studies demonstrated phase separation in films of calf (Discher et al., 1996) and porcine (Nag et al., 1998) surfactant, and in subfractions of calf surfactant from which specific components were removed (Discher et al., 1999). The more condensed of the two phases resembled LC DPPC in several qualitative respects. Our current results provide more quantitative information concerning the composition and structure of the domains. They also allow more specific conclusions concerning the effects of constituents other than the phospholipids on surfactant phase behavior. The hydrophobic surfactant proteins, for instance, lower the area of the nonfluorescent area when present with the phospholipids (Discher et al., 1999), suggesting that the proteins increase the partitioning of DPPC into the more expanded phase. The effects of the neutral lipids are even more dramatic. The phases that initially separate in both calf and porcine surfactant remix when compressed further. This effect is directly attributable to cholesterol, which apparently alters the phase diagram for the phospholipids to introduce a critical point (Discher et al., 1999). In light of recent evidence suggesting that the main LE–LC phase transition for DPPC itself lacks a critical point (Crane et al., 1999), the cholesterol presumably permeates the condensed domains and induces significant structural changes. Our results with PPL seem likely to be especially important for studies at the high surface pressures of particular interest for pulmonary surfactant. DPPC has long been considered crucial for the ability of surfactant films to reach these high pressures. The ability to monitor the spatial location of that compound in the multicomponent phospholipid mixture should be helpful in understanding the processes by which pulmonary surfactant forms stable films at high surface pressures.

The authors gratefully acknowledge the gift of extracted calf surfactant (Infasurf) by Dr. Edmund Egan of ONY, Inc., the guidance of Dr. William Vollmer of the Kaiser Center for Health Research concerning propagation of error, and helpful discussions with Dr. David Grainger of Colorado State University concerning work in progress. Heather Helming assisted in the preparation of samples of PPL. This research was supported by funds from the National Institutes of Health (HL 03502 and 54209), the Whitaker Foundation, and the American Lung Association of Oregon. B.M.D. was supported in part by a fellowship from the Tartar Trust. W.R.S. was supported as a predoctoral fellow by National Institutes of Health training grants in Biotechnology (GM 08437) and Molecular Biophysics (GM 08268). Page charges were provided in part by the friends and family of Vern McKee.

REFERENCES

Ames, B. N. 1966. Assay of inorganic phosphate, total phosphate and phosphatases. *Meth. Enzymol.* 8:115–118.

Bevington, P. R., and D. K. Robinson. 1992. Data Reduction and Error Analysis for the Physical Sciences. McGraw-Hill, New York. p. 46.

Crane, J. M., G. Putz, and S. B. Hall. 1999. Persistence of phase coexistence in dipalmitoyl phosphatidylcholine monolayers at high surface pressures. *Biophys. J.* 76:A60.

Discher, B. M., K. M. Maloney, D. W. Grainger, C. A. Sousa, and S. B. Hall. 1999. Neutral lipids induce critical behavior in interfacial monolayers of pulmonary surfactant. *Biochemistry.* 38:374–383.

Discher, B. M., K. M. Maloney, W. R. Schief, Jr., D. W. Grainger, V. Vogel, and S. B. Hall. 1996. Lateral separation of interfacial domains in films of pulmonary surfactant. *Biophys. J.* 71:2583–2590.

Frey, W., W. R. Schief, Jr., and V. Vogel. 1996. Two-dimensional crystallization of streptavidin studied by quantitative Brewster angle microscopy. *Langmuir.* 12:1312–1320.

Grainger, D. W., A. Reichert, H. Ringsdorf, and C. Salesse. 1989. An enzyme caught in action: direct imaging of hydrolytic function and domain formation of phospholipase A_2 in phosphatidylcholine monolayers. *FEBS Lett.* 252:73–82.

Hall, S. B., Z. Wang, and R. H. Notter. 1994. Separation of subfractions of the hydrophobic components of calf lung surfactant. *J. Lipid Res.* 35: 1386–1394.

Hénon, S., and J. Meunier. 1991. Microscope at the Brewster angle: direct observation of first-order phase transitions in monolayers. *Rev. Sci. Instr.* 62:936–939.

Hönig, D., and D. Möbius. 1991. Direct visualization of monolayers at the air–water interface by Brewster angle microscopy. *J. Phys. Chem.* 95: 4590–4592.

Hönig, D., G. A. Overbeck, and D. Möbius. 1992. Morphology of pentadecanoic acid monolayers at the air/water interface studied by BAM. *Adv. Mater.* 4:419–424.

Kahn, M. C., G. J. Anderson, W. R. Anyan, and S. B. Hall. 1995. Phosphatidylcholine molecular species of calf lung surfactant. *Am. J. Physiol.* 269: L567–L573.

Keough, K. M. W. 1992. Physical chemistry of pulmonary surfactant in the terminal air spaces. *In* Pulmonary Surfactant: From Molecular Biology to Clinical Practice. Elsevier Science Publishers, Amsterdam. 109–164.

Knobler, C. M. 1990. Recent developments in the study of monolayers at the air–water interface. *Adv. Chem. Phys.* 77:397–449.

Lipp, M. M., K. Lee, J. A. Zasadzinski, and A. J. Waring. 1996. Phase and morphology changes in lipid monolayers induced by SP-B protein and its amino-terminal peptide. *Science.* 273:1196–1199.

Lösche, M., E. Sackmann, and H. Möhwald. 1983. A fluorescence microscopic study concerning the phase diagram of phospholipids. *Ber. Bunsen-Ges. Phys. Chem.* 87:848–852.

Maruyama, T., G. Fuller, C. Frank, and C. Robertson. 1996. Flow-induced molecular orientation of a Langmuir film. *Science.* 274:233–235.

McConlogue, C. W., and T. K. Vanderlick. 1997. A close look at domain formation in DPPC monolayers. *Langmuir.* 13:7158–7164.

McConnell, H. M., L. K. Tamm, and R. M. Weis. 1984. Periodic structure in lipid monolayer phase transitions. *Proc. Natl. Acad. Sci. USA.* 81: 8249–8253.

Meller, P. 1988. Computer-assisted video microscopy for the investigation of monolayers on liquid and solid substrates. *Rev. Sci. Instr.* 59: 2225–2231.

Moy, V. T., D. J. Keller, H. E. Gaub, and H. M. McConnell. 1986. Long-range molecular orientational order in monolayer solid domains of phospholipids. *J. Phys. Chem.* 90:3198–3202.

Moy, V. T., D. J. Keller, and H. M. McConnell. 1988. Molecular order in finite two-dimensional crystals of lipid at the air–water interface. *J. Phys. Chem.* 92:5233–5238.

Nag, K., and K. M. W. Keough. 1993. Epifluorescence microscopic studies of monolayers containing mixtures of dioleoyl- and dipalmitoylphosphatidylcholines. *Biophys. J.* 65:1019–1026.

Nag, K., J. Perez-Gil, J. L. F. Ruano, L. A. D. Worthman, J. Stewart, C. Casals, and K. M. W. Keough. 1998. Phase transitions in films of lung surfactant at the air–water interface. *Biophys. J.* 74:2983–2995.

Notter, R. H., J. N. Finkelstein, and R. D. Taubold. 1983. Comparative adsorption of natural lung surfactant, extracted phospholipids, and artificial phospholipid mixtures to the air–water interface. *Chem. Phys. Lipids.* 33:67–80.

Peters, R., and K. Beck. 1983. Translational diffusion in phospholipid monolayers measured by fluorescence microphotolysis. *Proc. Natl. Acad. Sci. USA.* 80:7183–7187.

Schürch, S. 1982. Surface tension at low lung volumes: dependence on time and alveolar size. *Respir. Physiol.* 48:339–355.

Tabak, S. A., and R. H. Notter. 1977. A modified technique for dynamic surface pressure and relaxation measurements at the air–water interface. *Rev. Sci. Instr.* 48:1196–1201.

Takahashi, A., and T. Fujiwara. 1986. Proteolipid in bovine lung surfactant: its role in surfactant function. *Biochem. Biophys. Res. Comm.* 135:527–532.

Weidemann, G., and D. Vollhardt. 1995. Long range tilt orientational order in phospholipid monolayers: a comparison of the order in the condensed phases of dimyristoylphosphatidylethanolamine and dipalmitoylphosphatidylcholine. *Colloids Surf. A.* 100:187–202.

Weidemann, G., and D. Vollhardt. 1996. Long-range tilt orientational order in phospholipid monolayers: a comparative study. *Biophys. J.* 70: 2758–2766.